

Advancing super resolution microscopy for quantitative in-vivo imaging of chromatin nanodomains

Clayton W. Seitz
PhD Candidate (IUI), MS (UChicago)

August 26, 2024

Outline

Introduction to fluorescence nanoscopy

Contemporary approaches to fluorescence nanoscopy

Enhanced nanoscopy with deep generative models

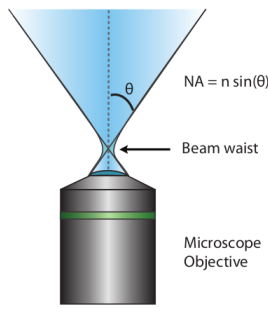
Enhanced nanoscopy with a single photon avalanche diode array

Super-resolution of nucleosome nanodomains *in-vivo*

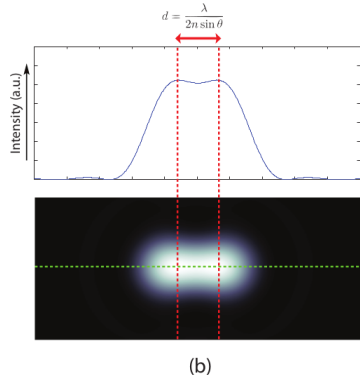
Introduction to fluorescence nanoscopy

Fluorescence microscopy and the diffraction limit

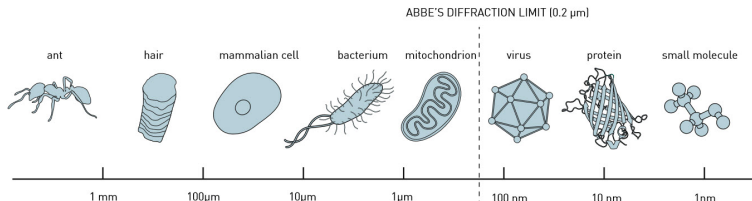
Minimal resolvable distance $d \sim \lambda$



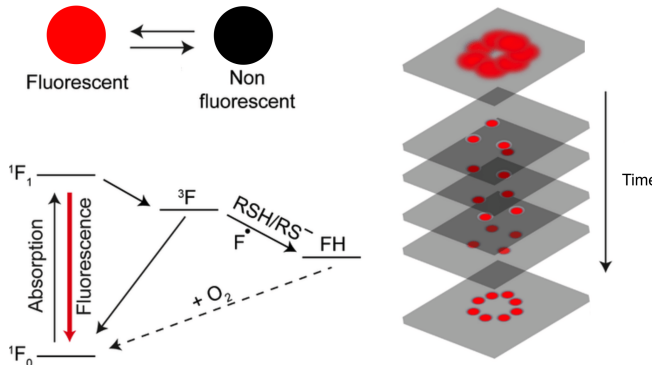
(a)



(b)

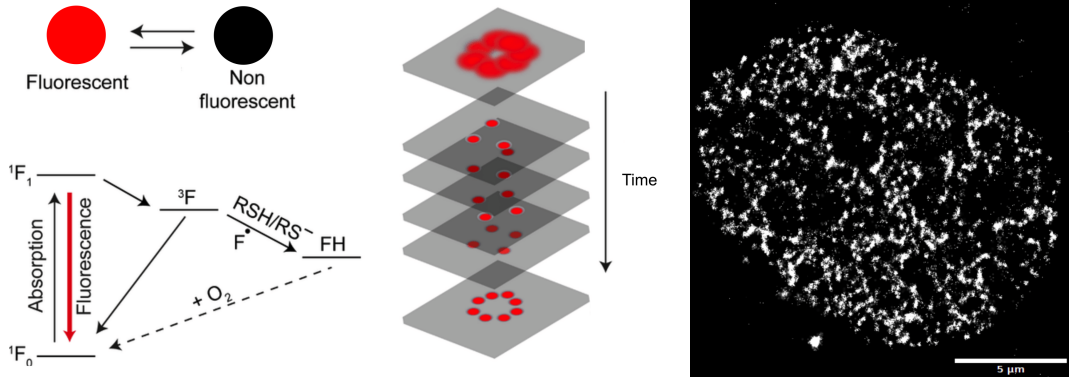


Stochastic optical reconstruction microscopy (STORM)



- ▶ STORM and similar nanoscopy techniques are diffraction-unlimited
- ▶ Photoswitching enables resolution of emitters below the diffraction limit

Stochastic optical reconstruction microscopy (STORM)



- ▶ STORM and similar nanoscopy techniques are diffraction-unlimited
- ▶ Photoswitching enables resolution of emitters below the diffraction limit

Nanoscopy by localizing isolated fluorescent emitters

Modeling the point spread function permits sub-pixel localization

$$\mu_k = i_0 \int \int O(u, v) dudv + \lambda$$

$$i_0 = g_k \eta \zeta \Delta$$

g_k – pixel gain

η – quantum efficiency

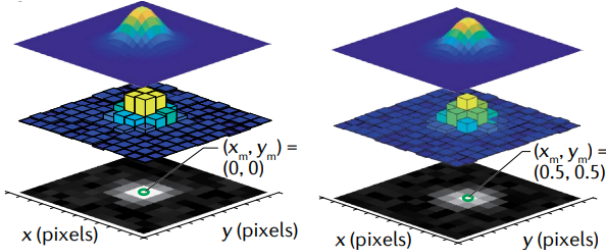
ζ – photon emission rate

Δ – exposure time

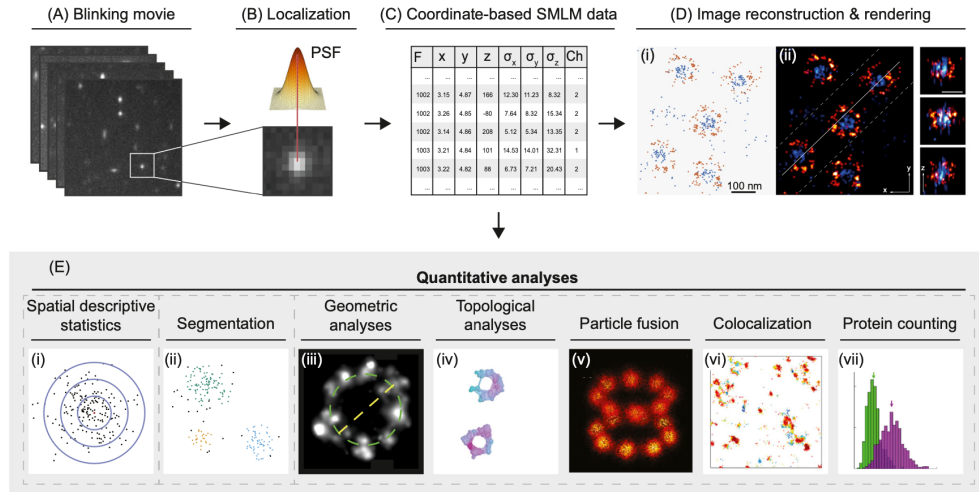
λ – background rate

Maximum likelihood localization:

$$\theta^* = \operatorname{argmax}_{\theta} \prod_k p(\mathbf{x}_k | \theta) = \operatorname{argmin}_{\theta} - \sum_k \log p(\mathbf{x}_k | \theta)$$

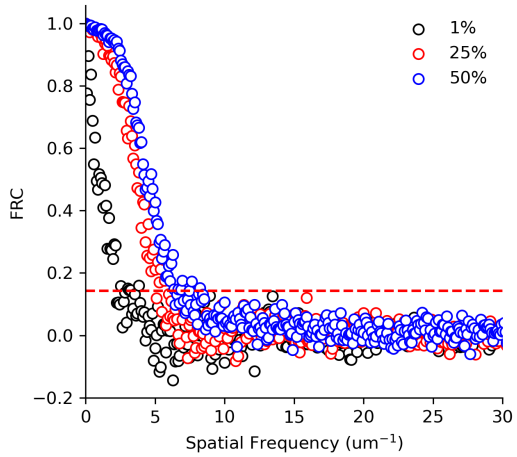
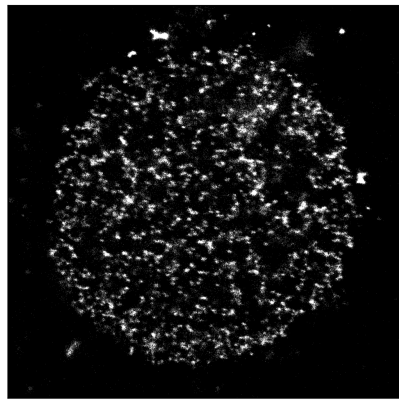


Applications of single molecule localization microscopy



Wu et al. Trends in Cell Biology. 30 (2020)

How do we define resolution in localization microscopy?



More samples → higher spatial/temporal resolution

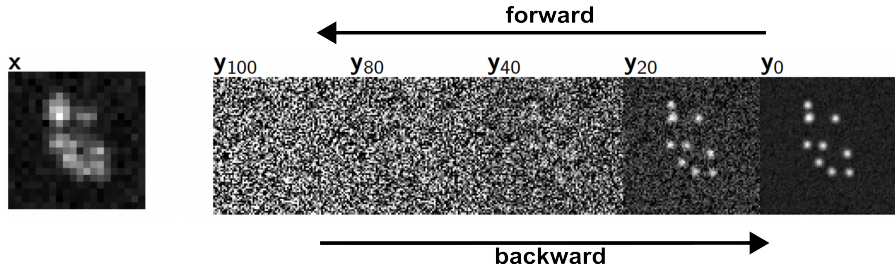
How to relax the density limit in localization microscopy?

Contemporary approaches to fluorescence nanoscopy

Bayesian image restoration with diffusion models

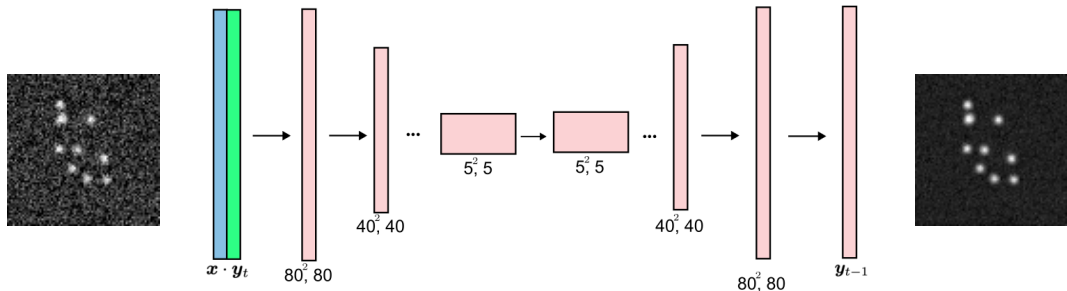
Inference of a high resolution image \mathbf{y} from low resolution \mathbf{x} is approached by modeling a distribution $p_\psi(\mathbf{y}|\mathbf{x})$ with a diffusion model

$$q(\mathbf{y}_t | \mathbf{y}_{t-1}) = \mathcal{N}\left(\sqrt{1 - \beta_t} \mathbf{y}_{t-1}, \beta_t I\right)$$



$$p_\psi(\mathbf{y}_{t-1} | \mathbf{y}_t, \mathbf{x}) = \mathcal{N}(\mu_\psi(\mathbf{y}_t, \gamma_t), \beta_t I)$$

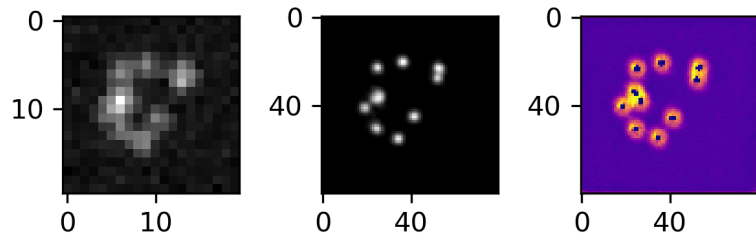
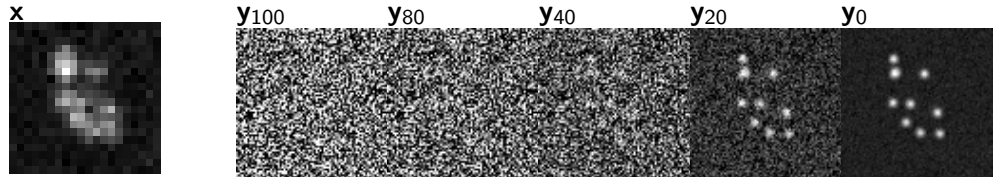
Bayesian image restoration with diffusion models



A deep neural network estimates the gradient of the reverse process

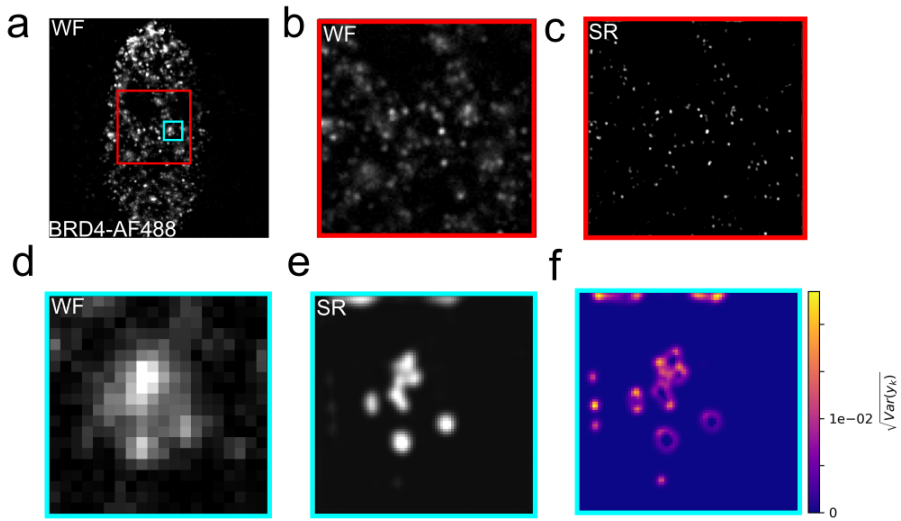
$$\mathbf{y}_{t-1} = \frac{1}{\sqrt{1 - \beta_t}} (\mathbf{y}_t + \beta_t s_\psi(\mathbf{y}_t)) + \sqrt{\beta_t} \xi \quad \xi \sim \mathcal{N}(0, I)$$

Bayesian image restoration with diffusion models

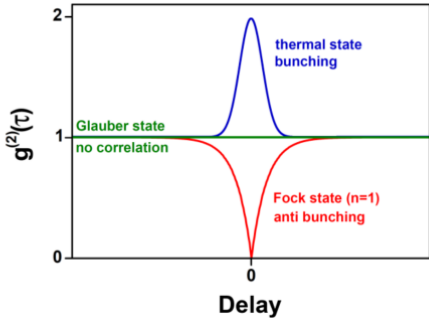
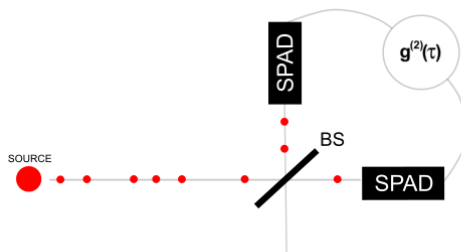


Estimation of pixel-wise uncertainty in the high resolution y

Super resolution of BRD4 in a HeLa cell



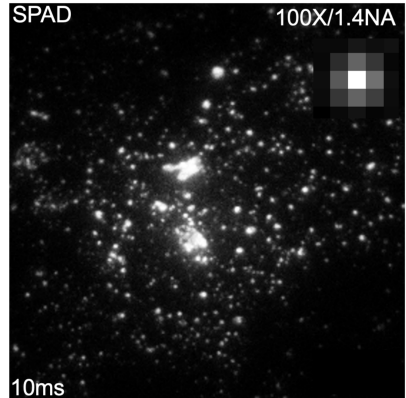
The Hanbury Brown and Twiss Effect



$$g^{(2)}(\tau) = \frac{\langle n(t)n(t + \tau) \rangle}{\langle n(t) \rangle^2}$$

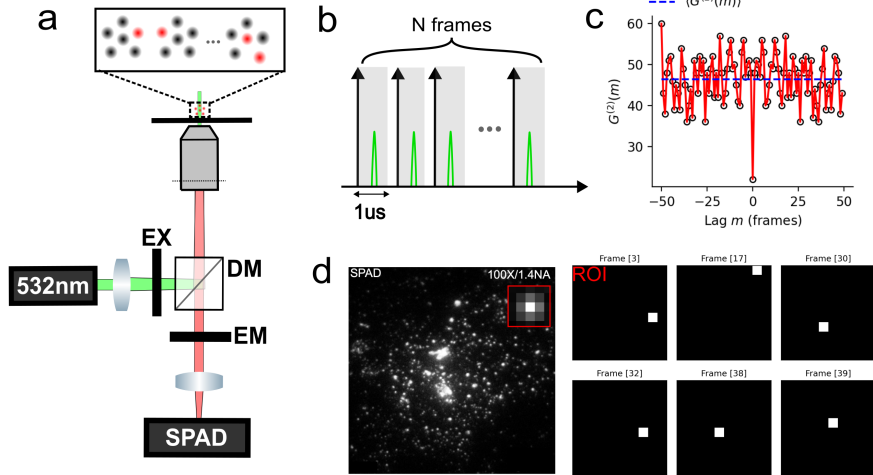
- ▶ Single photon sources (such as a fluorescent dye) exhibit antibunching
- ▶ Magnitude of $g^{(2)}(0)$ "dip" depends on the number of fluorescent emitters
- ▶ Provides a means of counting fluorescent emitters

Widefield photon counting with a SPAD array

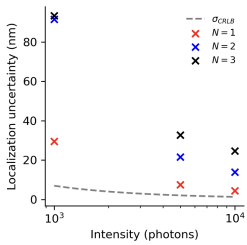
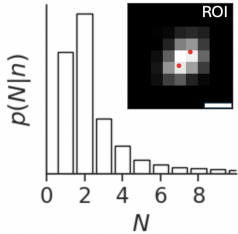
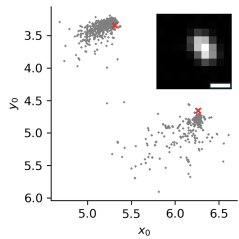
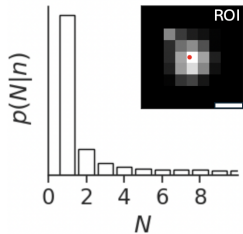


- ▶ Spatial resolution of photon counts
- ▶ Fast exposures as low as 20 nanoseconds

Imaging Qdot655 photon by photon



Constrained multi-emitter localization with photon counting

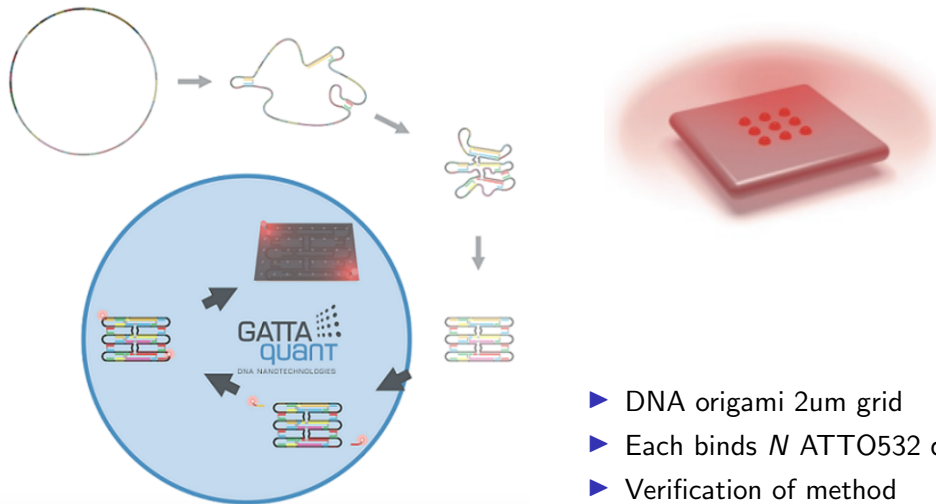


Posterior distribution on (N, ζ) :

$$p(N, \zeta|n) \propto p(n|N, \zeta)p(\zeta)$$

- ▶ MAP estimation on N
- ▶ Parameterization of multi-emitter fitting
- ▶ Approaches σ_{CRLB} for $N = 1$

Counting ATTO532 dye bound to DNA origamis

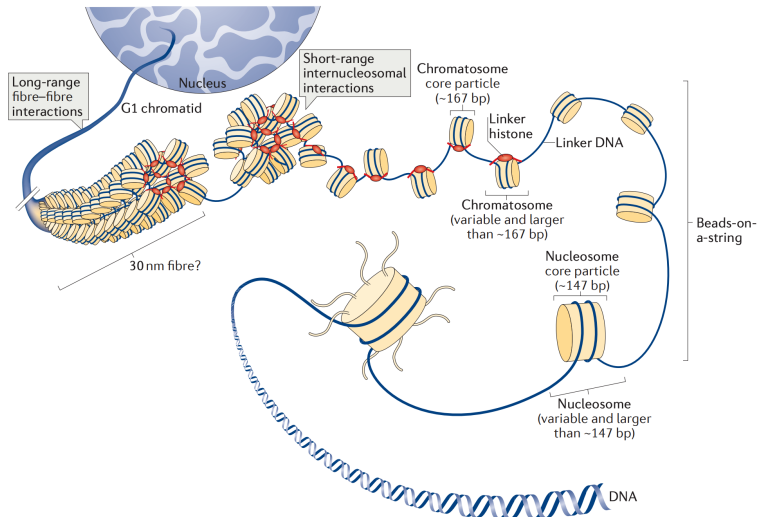


- ▶ DNA origami 2um grid
- ▶ Each binds N ATTO532 dyes
- ▶ Verification of method

Courtesy of GATTAquant DNA Nanotech

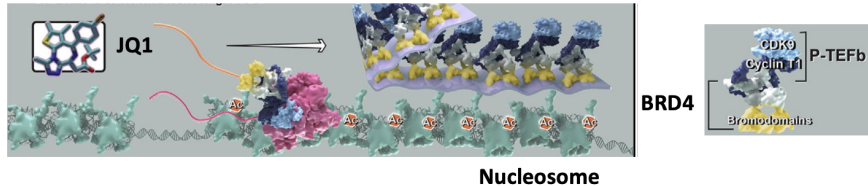
Super-resolution of nucleosome nanodomains *in-vivo*

Hierarchical structure of chromatin

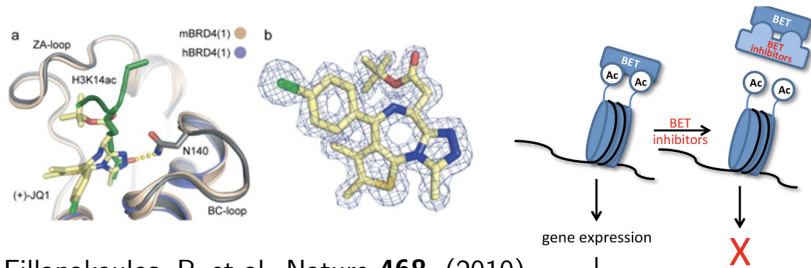


Fyodorov, D. et al. Nat Rev Mol Cell Biol **19**, (2018).

Bromodomain protein 4 (BRD4) binds acetylated chromatin

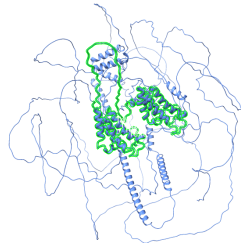
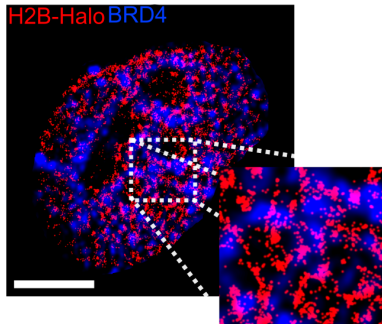


Zheng, B. et al. Molecular Cell **16**, (2023).



Fillapakoulos, P. et al. Nature **468**, (2010).

Bromodomain protein 4 (BRD4) binds acetylated chromatin

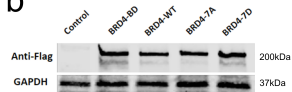


BRD4 phosphorylation state is necessary for maintenance of chromatin structure

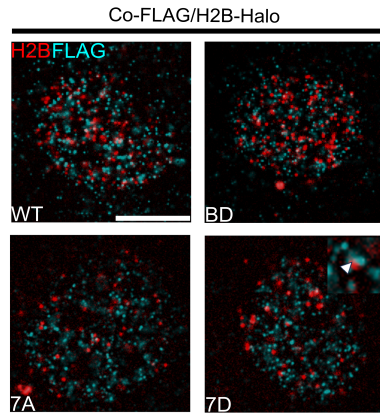
a



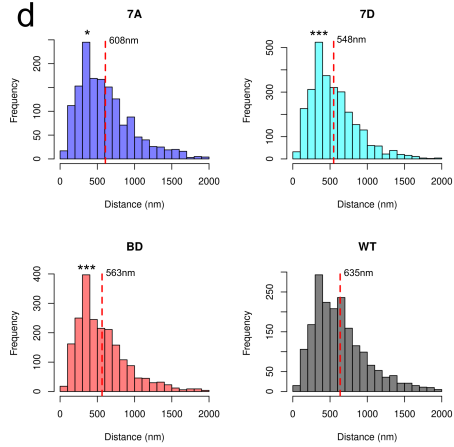
b



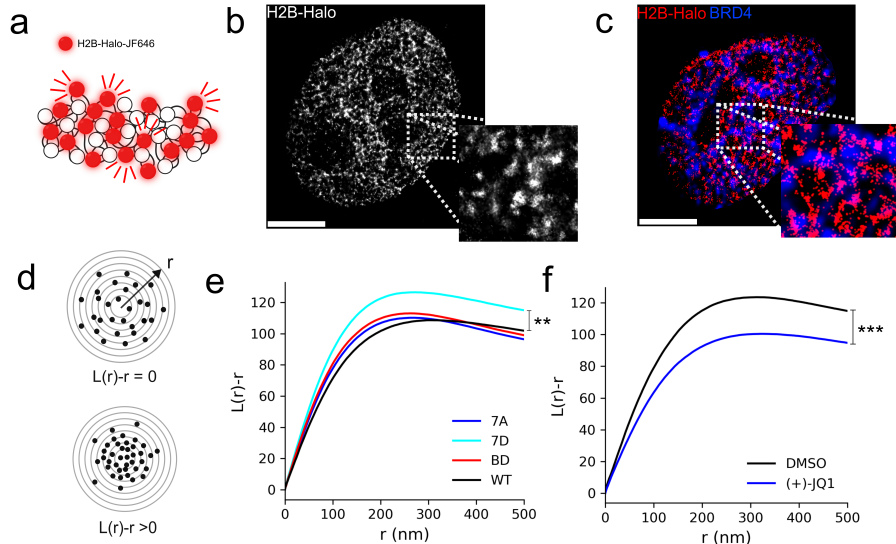
c



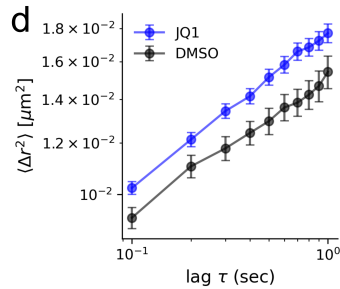
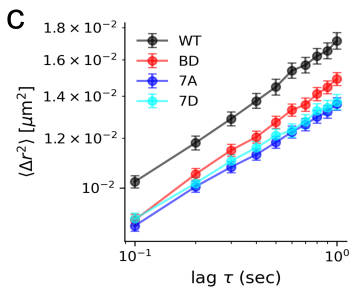
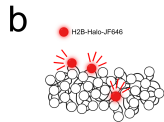
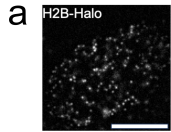
d



BRD4 phosphorylation state is necessary for maintenance of chromatin structure

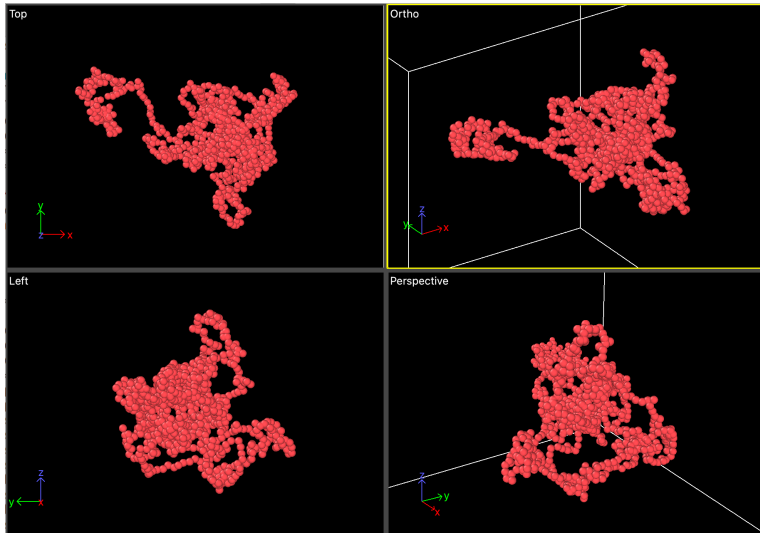


Multivalent chromatin binding reduces chromatin mobility



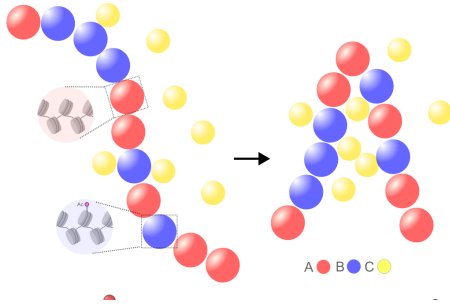
Experiment: $D_{W\tau} - D_{7D} \approx 10^{-3} \mu\text{m}^2/\text{s}, \gamma = 10^{-6}$

Coarse grained molecular dynamics of chromatin at 310K

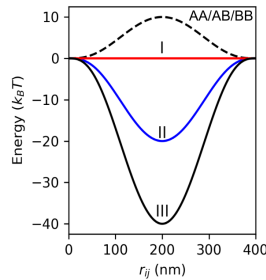


Coarse grained molecular dynamics of chromatin binders at 310K

a



b

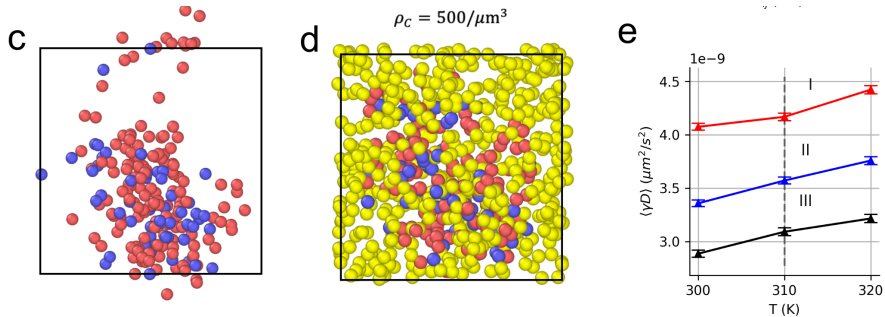


100kb chromatin chains interact with binders via the potential

$$U_{ij} = \epsilon \left(1 - \left(\frac{|r_{ij}|}{R_0} \right)^2 \right)^3$$

- ▶ A (B) type particles represent unacetylated (acetylated) chromatin beads
- ▶ BRD4-like C particles bind B type particles with variable energies

Multivalent chromatin binding reduces chromatin mobility



Integrate Brownian dynamics: $\dot{r} = \gamma^{-1} \nabla U + \sqrt{2k_B T} \gamma^{-1/2} \xi$ $\gamma = 10^{-6}$

Stochastic forcing is a delta-correlated white-noise
 $\xi \sim \mathcal{N}(0, 1)$, $\langle \xi(t) \xi(t + \tau) \rangle = \delta(\tau)$

Acknowledgements



(left to right) Charles Park, Garrick Chang, Jing Liu, David Buchanan, Mengyuan Liu, Hailan Ma



Norbert Scherer



Donghong Fu

Thank you!